Dariusz STANDO
Marian P. KAŹMIERKOWSKI

OPTIMAL SWITCHING SEQUENCE – MODEL PREDICTIVE FLUX CONTROL OF THREE-LEVEL INVERTER-FED INDUCTION MOTOR DRIVE

ABSTRACT *The paper presents a novel model predictive torque control scheme for three-level inverter-fed sensorless induction motor drive operated in wide speed region including field weakening. Among the important features of the developed drive are: very high dynamics, constant switching frequency and no need to adjust weighting factors in the cost function. The theoretical principles of the used optimal switching sequence predictive control methods are discussed. The experimental results measured on 50 kW drive validate performances of the proposed predictive control system.*

Keywords: *Model predictive control, Induction motor drives, three-level NPC inverters*
DOI: 10.5604/01.3001.0013.0183

1. INTRODUCTION

In recent years, model predictive control (MPC) strategies are extensively developed for control in power electronics and AC drives mainly thanks to following advantages:

- MPC is general strategy which can be applied to a variety of systems,
- it implements on-line optimization,
- cost function serves as a single controller for many variables,
- one control loop,
- easy inclusion of nonlinearities in the model,
- simple treatment of constraints,
- high dynamics,
- easy inclusion of modifications and extensions for specific applications.

Dr. Dariusz STANDO[1, 2] and Professor Marian P. KAŹMIERKOWSKI[2]
darek.stando@gmail.com, mpk@isep.pw.edu.pl

[1] En-Tran Tech Sp. z o.o., Szachowa 1/853, 04-894 Warsaw, Poland
[2] Electrotechnical Institute, M. Pożaryskiego 28, 04-703 Warsaw, Poland

To follow the needs of power electronics, a number of MPC methods have been developed that can be classified as shown in Figure 1. The Prediction method, which has so far found the largest number of applications in power electronics is *Optimal Switching Vector – Model Predictive Control* (OSV-MPC) [1 – 6], [13]. This method is characterized by a variable switching frequency and the problem of selecting weights of cost function. In most applications for IM drives, the cost function consists of torque and stator flux amplitude errors, which differs in terms of units and size. In this case, to achieve the desired properties of the drive, it is necessary to select appropriate weighting factors. Selection of weight factors, however, is not trivial task due to the lack of theoretical procedures and usually the trial and error method is performed. In the literature, you can find solutions to solve this problem [1], [5], [7 – 10], but these methods are quite complicated. In addition, beyond the problem of selecting the weights in the cost function, the OSV-MPC has more disadvantages such as: high torque ripple and high sampling frequency. Therefore, this paper focus on the application of MPC to three-level NPC inverter fed induction motor drive, considering the group of finite control set (FCS) with *Optimal Switching Sequence* (OSS-MPC) which solves the above problems of classic OSV-MPC and at the same time retains the advantage of high dynamics of torque regulation.

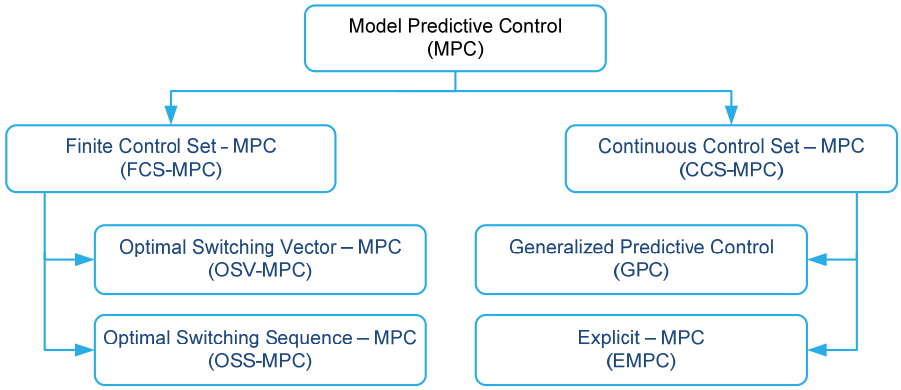

Fig. 1. Classification of the MPC methods used in power electronics and AC drives [11]

2. MATHEMATICAL MODEL OF INDUCTION MOTOR

Mathematical model of the idealized induction motor (IM) is based on *complex space vectors*, which can be defined in the stationary $\alpha\beta$ coordinates [12]:

$$\mathbf{V_S} = \mathbf{I_S} \cdot R_S + \frac{d\boldsymbol{\Psi}_S}{dt} \tag{1a}$$

$$\mathbf{0} = \mathbf{I_R} \cdot R_R + \frac{d\boldsymbol{\Psi}_R}{dt} - j \cdot p_b \cdot \Omega_m \cdot \boldsymbol{\Psi}_\mathbf{R} \tag{1b}$$

$$\boldsymbol{\Psi}_\mathbf{S} = \mathbf{I_S} \cdot L_S + \mathbf{I_R} \cdot L_M \tag{1c}$$

$$\boldsymbol{\Psi}_\mathbf{R} = \mathbf{I_R} \cdot L_R + \mathbf{I_S} \cdot L_M \tag{1d}$$

$$\frac{d\Omega_m}{dt} = \frac{1}{J} \cdot \left[\frac{3}{2} \cdot p_b \cdot \mathrm{Im}(\boldsymbol{\Psi}_\mathbf{S}^* \cdot \mathbf{I_S}) - M_L\right] \tag{1e}$$

Where $\mathbf{V_S} = (V_{S\alpha}, V_{S\beta})$, $\mathbf{I_S} = (I_{S\alpha}, I_{S\beta})$, $\boldsymbol{\Psi}_\mathbf{S} = (\Psi_{S\alpha}, \Psi_{S\beta})$ are the stator voltage vector, the stator current vector and stator flux vector, respectively. $\mathbf{I_R} = (I_{R\alpha}, I_{R\beta})$, $\boldsymbol{\Psi}_\mathbf{R} = (\Psi_{R\alpha}, \Psi_{R\beta})$ are the rotor current vector and rotor flux vector, respectively. Ω_m – denotes the rotor electrical angular speed. R_S, R_R, L_S, L_R, L_M – are the stator resistance, rotor resistance, stator inductance, rotor inductance and main inductance, respectively. Lastly, p_b denotes the pair of poles, J the moment of inertia, $\boldsymbol{\Psi}_\mathbf{S}^*$ conjugate stator flux vector, and M_L – is the load torque.

3. MODEL OF THREE-LEVEL INVERTER

Figure 2 depicts the three-phase three-level neutral point clamped (3L-NPC) voltage source inverter (VSI). Each of the inverter legs can generate three voltage levels: $V_{dc}/2$, 0 and $-V_{dc}/2$. This is accomplished by means of three combinations of switch states assigned the number: 2, 1 or 0, where:

State 2:

$$V_x = V_{dc},$$

State 1:

$$V_x = V_{dc}/2, \tag{2}$$

State 0:

$$V_x = 0,$$

for

$$x = A, B, C.$$

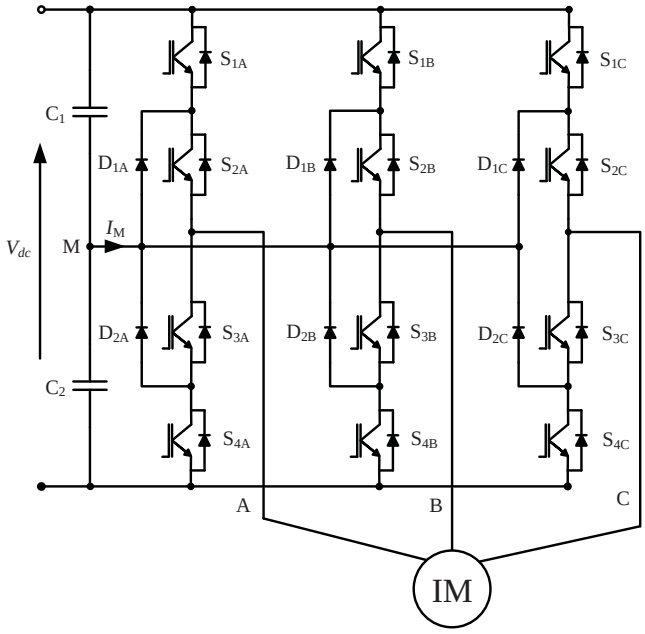

	0	1	2
S_{1X}	off	off	on
S_{2X}	off	on	on
S_{3X}	on	off	off
S_{4X}	on	on	off

Fig. 2. Circuit of a three-level NPC-inverter and switch states table

Taking into account the available combinations of switch states of particular legs, a three-phase three-level converter generates 27 basic vectors, of which twenty-four are active states (six of them are redundant states) and three are zero states:

- 3 zero (000, 111, 222)
- 12 short (100, 211, 110, 221, 010, 121, 011, 122, 001, 112, 101, 212)
- 6 medium (210, 120, 021, 012, 102, 201)
- 6 long (200, 220, 020, 022, 002, 202).

The state of a given vector is determined in three positions. The first relates to the switches in the leg of phase A, the second to the switches in phase B, the third to the switches in phase C. The switching state vector has the following form:

$$\mathbf{V}_{ABC} = [V_A, V_B, V_C]^T \in V_{27} := \{000, 001 \ldots 221, 222\}. \tag{3}$$

The voltage applied to the IM terminals in orthogonal coordinates $\alpha\beta$ is – for neglected fluctuations of the neutral point potential – given by:

$$\mathbf{V}_{S\alpha\beta} = (V_{dc}/2)\, \mathbf{K}\, \mathbf{V}_{ABC}, \tag{4}$$

where **K** is reduced Clarke transformation:

$$\mathbf{K} = \frac{2}{3}\begin{Bmatrix} 1 & -\frac{1}{2} & -\frac{1}{2} \\ 0 & \frac{\sqrt{3}}{2} & -\frac{\sqrt{3}}{2} \end{Bmatrix}. \tag{5}$$

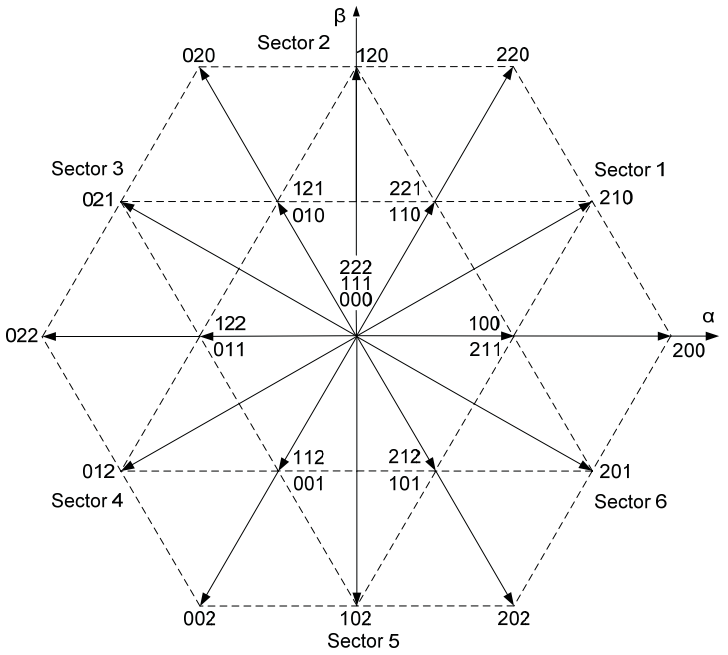

Fig. 3. Representation of output voltage of a three-level inverter as space vectors and division of the α-β plane into sectors by long vectors and regions by short and medium vectors

4. PREDICTIVE STATOR FLUX VECTOR CONTROL WITH OPTIMAL SWITCHING SEQUENCE (OSS-MPFC)

The developed Optimal Switching Sequence-Model Predictive Flux Control (OSS-MPFC) control structure is implemented in accordance with the algorithm presented in Figure 4 and Figure 5. In this system, the control is based on a predictive model and one controller in the form of a cost function with optimization block.

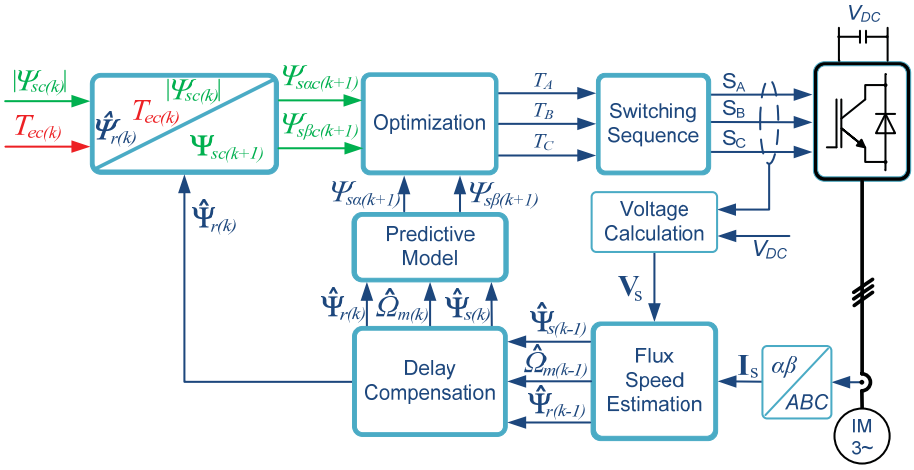

Fig. 4. Block scheme of the model predictive stator flux control method (OSS-MPFC)

4.1. Predictive model

The bases of the predictive control are models of the IM and the 3L-VSI. The predictive model of the IM was formulated on basis of the IM equations in a stationary $\alpha\beta$ system (1) transformed into the state equations of the stator flux and current.

$$\frac{d\boldsymbol{\Psi}_\mathrm{s}}{dt} = \mathbf{V}_\mathrm{s} - \mathrm{R_s}\mathbf{I}_\mathrm{s} \tag{6}$$

After transformation using the Euler method, a discrete form of Eq. (6) was obtained as:

$$\boldsymbol{\Psi}_s(k+1) = \boldsymbol{\Psi}_s(k) + \left[\mathbf{V}_s(k) - R_s\mathbf{I}_s(k)\right]\cdot T_s \tag{7}$$

where: k – sampling step, T_s – sampling time.

Taking into account set of equations (1) one obtains the predictive model of the IM:

$$\boldsymbol{\Psi}_\mathrm{s}(k+1) = \boldsymbol{\Psi}_\mathrm{s}(k) + \left[\frac{R_s L_m}{\sigma L_s L_r}\boldsymbol{\Psi}_\mathrm{r}(k) - \frac{R_s}{\sigma L_s}\boldsymbol{\Psi}_\mathrm{s}(k) + \mathbf{V}_\mathrm{s}(k)\right] T_s \tag{8a}$$

$$\boldsymbol{\Psi}_\mathrm{r}(k+1) = \boldsymbol{\Psi}_\mathrm{r}(k) + \left[\frac{R_r L_s}{L_m}\mathbf{I}_\mathrm{s}(k) - \frac{R_r}{L_m}\boldsymbol{\Psi}_\mathrm{s}(k) + \mathrm{j}p_b\Omega_m\boldsymbol{\Psi}_\mathrm{r}(k)\right] T_s \tag{8b}$$

where σ is total leakage factor.

4.2. Predictive controller – cost function

One of the most important advantages of predictive control is the possibility to use a cost function as a regulator. In the discussed case it can be defined as:

$$J = (\Psi_{s\alpha c}(k+1) - \Psi_{s\alpha}(k+1))^2 + \left(\Psi_{s\beta c}(k+1) - \Psi_{s\beta}(k+1)\right)^2 \tag{9}$$

In this form it is used to determine the optimal sector and then the region. In the first step, the set of stator flux in the $\alpha\beta$ stationary system is determined. For this purpose, the dependence of the phase angle between the stator and rotor flux (so called torque angle δ) was used. During no-load operation, the torque angle is equal to zero, whereas when the torque appears on the motor shaft it is directly proportional to the second component of equation (11). The first part of the equation results from the currently estimated position of the rotor flux $\gamma_{sr(k)}$. It is also necessary to take into account the effect of prediction, and therefore the desired position of the rotor flux at the application instant of the predicted switch states. This was done according to equation (10) taking into account that the time constant of the rotor circuit is much greater than the stator circuit time constant. Thanks to this, it can be assumed that the increment of the rotor flux angle is the same as in the previous period.

$$\gamma_{sr}(k+1) = \gamma_{sr}(k) + \omega_{sr}T_s \tag{10}$$

$$\gamma_{ssc}(k+1) = \gamma_{sr}(k+1) + \arcsin\left(\frac{2\left(L_s L_r - L_M^2\right)T_{ec}(k)}{p_b m_s L_M \Psi_s(k)\Psi_r(k)}\right) \tag{11}$$

$$\boldsymbol{\Psi}_{sc}(k+1) = |\boldsymbol{\Psi}_{sc}(k)|e^{j\gamma_{ssc}(k+1)} \tag{12}$$

this gives the command values of the stator flux αβ components:

$$\Psi_{s\alpha c}(k+1) = \Psi_{sc}\cos\left(\gamma_{ssc}(k+1)\right) \tag{13a}$$

$$\Psi_{s\beta c}(k+1) = \Psi_{sc}\sin\left(\gamma_{ssc}(k+1)\right) \tag{13b}$$

In the next step, the optimal sector is set, in which there is a wanted vector minimizing the cost functions. As result, the number of calculated values of the cost function is reduced from 18 of available vectors (excluding redundant vectors) to 10. This is accomplished by pre-determining the cost function for the longest vectors, and then finding the minimum sum of the cost functions of two neighbouring vectors. Each pair of vectors represents one of the six sectors as shown in Figure 3. After identifying the optimal sector in the next step, the cost functions are calculated to give the

remaining medium and short vectors within it. Then the optimal region is determined, i.e. the one in which the wanted vector is located. This process is similar to the selection of the optimal sector with the fact that in this case a minimum of the sum of three cost functions for neighbouring vectors representing the respective regions is sought.

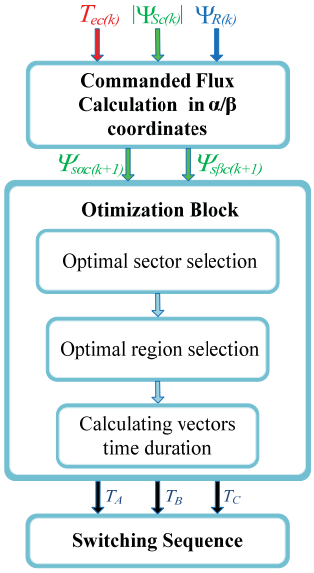

Fig. 5. Flow diagram of the OSS-MPFC control algorithm

After determining the region in which the voltage vector is located we were looking for, we can calculate the switching times of each of the three vectors representing the sector. This is carried out in accordance with the idea presented in Figure 6 and Equation 14.

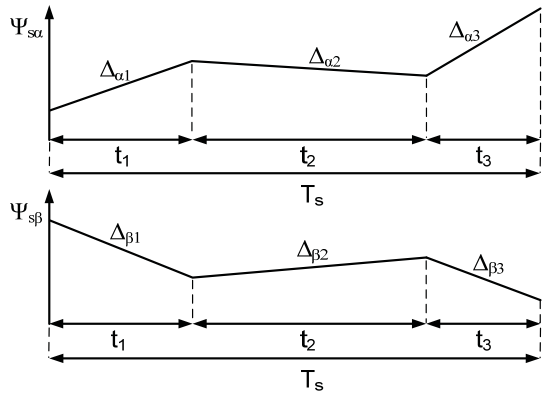

Fig. 6. Changes in the *αβ* components of the stator flux as a result of the application of three voltage vectors during one sampling period

$$J = \left(\Psi_{S\alpha c(k+1)} - \Psi_{S\alpha(k)} - (\Delta_{\alpha 1} t_1 + \Delta_{\alpha 2} t_2 + \Delta_{\alpha 3}(1 - t_1 - t_2)\right)^2 + \\ +(\Psi_{S\beta c(k+1)} - \Psi_{S\beta(k)} - (\Delta_{\beta 1} t_1 + \Delta_{\beta 2} t_2 + \Delta_3(1 - t_1 - t_2))^2 \quad (14)$$

After calculating partial derivatives with respect to t_1 and t_2 in accordance with the condition (15), we obtain formulas for optimal switching times (16)-(18)

$$\begin{cases} \frac{\partial J}{\partial t_1} = 0 \\ \frac{\partial J}{\partial t_2} = 0 \end{cases} \quad (15)$$

$$t_1 = \begin{bmatrix} \left(\Psi_{S\alpha c(k+1)} - \Psi_{S\alpha(k)} - \Delta_{\alpha 3}\right)\left(x_{\alpha 13} x_{\beta 23}^2 - x_{\alpha 23} x_{\beta 13} x_{\beta 23}\right) \\ +\left(\Psi_{S\beta c(k+1)} - \Psi_{S\beta(k)} - \Delta_{\beta 3}\right)\left(x_{\beta 13} x_{\alpha 23}^2 - x_{\beta 23} x_{\alpha 13} x_{\alpha 23}\right) \end{bmatrix} \\ /\left(x_{\alpha 13} x_{\beta 23} - x_{\alpha 23} x_{\beta 13}\right)^2 \quad (16)$$

$$t_2 = \begin{bmatrix} \left(\Psi_{S\alpha c(k+1)} - \Psi_{S\alpha(k)} - \Delta_{\alpha 3}\right)\left(x_{\alpha 23} x_{\beta 13}^2 - x_{\alpha 13} x_{\beta 13} x_{\beta 23}\right) \\ +\left(\Psi_{S\beta c(k+1)} - \Psi_{S\beta(k)} - \Delta_{\beta 3}\right)\left(x_{\beta 23} x_{\alpha 13}^2 - x_{\beta 13} x_{\alpha 13} x_{\alpha 23}\right) \end{bmatrix} \\ /\left(x_{\alpha 23} x_{\beta 13} - x_{\alpha 13} x_{\beta 23}\right)^2 \quad (17)$$

where:

$$x_{\alpha 13} = \Delta_{\alpha 1} - \Delta_{\alpha 3},\ x_{\alpha 23} = \Delta_{\alpha 2} - \Delta_{\alpha 3},\ x_{\beta 13} = \Delta_{\beta 1} - \Delta_{\beta 3},\ x_{\beta 23} = \Delta_{\beta 2} - \Delta_{\beta 3}$$

$$t_3 = 1 - t_1 - t_2 \quad (18)$$

The full flow diagram of the OSS-MPFC algorithm is shown in Figure 5.

5. EXPERIMENTAL VERIFICATION

5.1. Laboratory test stand

Laboratory tests were carried out in the Electrotechnical Institute (IEL) for the STDA 200LU traction machine, which parameters are shown in the Table 1 below. The sample rate of the DSPACE 1103 control card was 4 kHz.

TABLE 1
Parameters of the IM type STDA 200LU

IM STDA 200LU			
P_N	50 kW	R_S	64,5 mΩ
U_N	3 x 380	R_R	46,3 mΩ
I_N	88 A	L_S	25,217 mH
f_N	65 Hz	L_R	25,137 mH
T_{eN}	249 Nm	L_M	24,75 mH
p_b	2	J	10 gm^2

Fig. 7. View of the laboratory three-phase three-level 55 kVA inverter

5.2. Results of laboratory tests in steady-states

The oscillograms of steady-state operation of the OSS-MPFC controlled IM drive with constant speed 1300 rpm/min at nominal stator flux is shown in Figure 8. It can be observed typical 3-level phase to phase voltage and near sinusoidal, not distorted, shape of the stator flux and phase current.

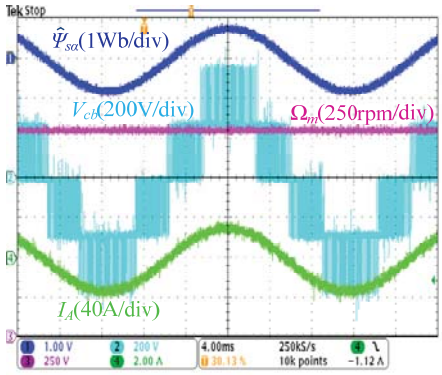

Fig. 8. No load steady-state operation at 1300 rpm/min

5.3. Results of laboratory and simulation tests in dynamic states

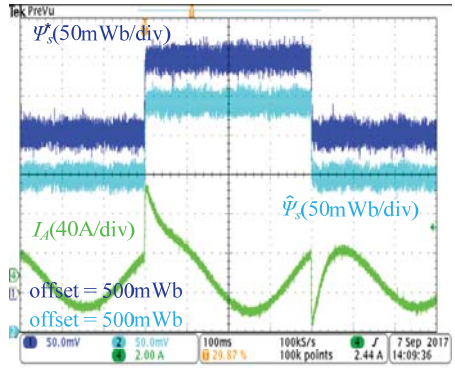

Fig. 9. Experimental results for step in the amplitude of stator flux 0.7→0.8→0.7 Wb

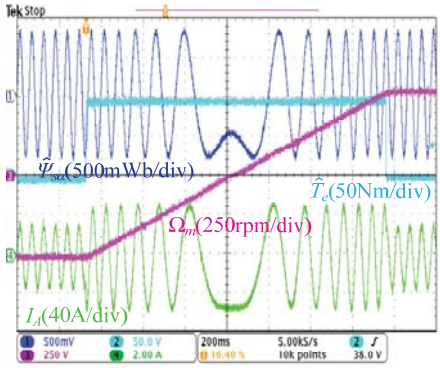

Fig. 10. Experimental results for speed reversal -500→500 rpm/min under torque step change -100→100 Nm

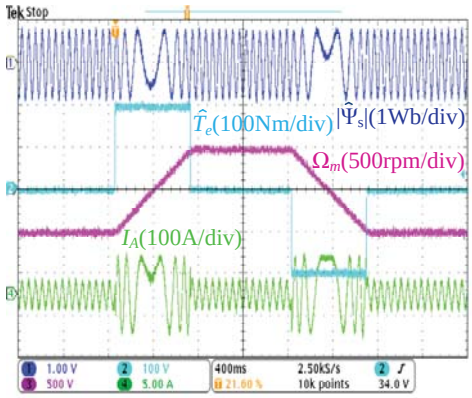

Fig. 11. Experimental results for speed reversal -500→500 rpm/min under torque step change -200→200 Nm

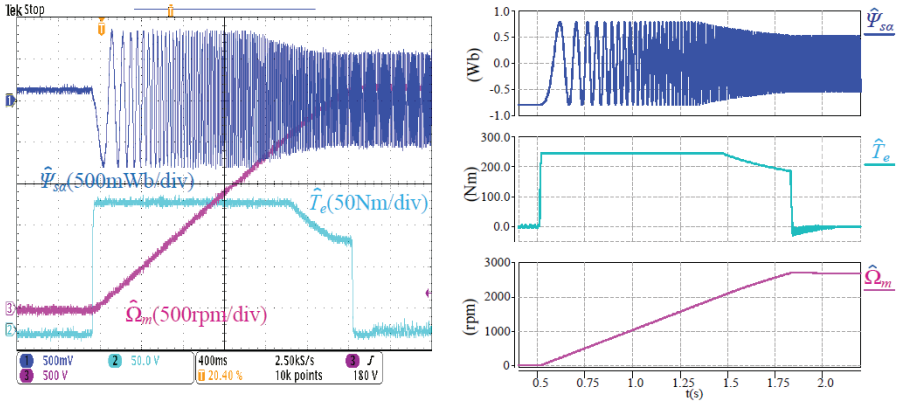

Fig. 12. Start up to 2700 rpm/min including field weakening region Left: experimental, Right: simulated

The excellent dynamic performances of stator flux and torque control are presented in Figures 9 – 12, respectively. During the test the stator flux has been changed stepwise (Fig. 9), but the boundary of changes were limited by current measurement probe. Note, that in torque tests (Fig. 10 and 11) speed is not controlled, because the electrical vehicle drives use mostly only the torque control. The experimental and simulated start-up including field weakening range is presented in Figure 12 which shows that in the constant voltage region the stator flux amplitude and torque are reduced.

6. SUMMARY AND CONCLUSIONS

The paper presents the novel *Optimal Switching Sequence-Model Predictive Flux Control (OSS-MPFC)* strategy for three-level inverter-fed induction motor drives suited for electrical vehicles. Contrary to the most popular classical Optimal Switching Vector – Model Predictive Flux Control (OSS-MPFC) strategy, proposed method applies not only one voltage vector, but the optimal sequence of three voltage vectors in every sampling period. The optimal sequence of voltage vectors is selected using cost function based on stator flux error (Eq. 9) which guarantees following properties:

- constant switching frequency operation of the three-level inverter (similar as in the space vector modulation),
- reduced torque and current ripple comparable with cascade controlled drives (FOC, DTC-SVM [1], [12]),
- elimination of weighting factors selection in the cost function thanks to use only stator flux error (not torque error),
- maintaining high dynamics typical for predictive control strategies,
- operation in field weakening region.

The only condition for taking into operation the drive system is the knowledge of the IM parameters. There is no need to select any parameters of regulators, if the drive operates in torque control loop. In the cases when the speed control loop is required, only design of the PI speed controller is necessary.

LITERATURE

1. Rodriguez J. and. Cortes P: "Predictive Control of Power Converters and Electrical Drives", *Wiley-IEEE Press*, 2012.
2. Geyer T. and Quevedo D. E.: "Multistep Finite Control Set Model Predictive Control for Power Electronics", *IEEE Trans. Power Electron*., vol. 29, no. 12, pp. 6836–6846, Dec. 2014.
3. Abu-Rub H., Guzinski J., Krzeminski Z. and Toliyat H. A.: "Speed observer system for advanced sensorless control of induction motor", *IEEE Trans. Energy Convers*., vol. 18, no. 2, pp. 219–224, Jun. 2003.
4. Rodriguez J. et al.: "Predictive Current Control of a Voltage Source Inverter". I*EEE Trans. Ind. Electron*., vol. 54, no. 1, pp. 495–503, Feb. 2007.
5. Rojas C. A., Rodriguez J., Villarroel F., Espinoza J. R., Silva C. A., and Trincado M.: "Predictive Torque and Flux Control Without Weighting Factors", *IEEE Trans. Ind. Electron.*, vol. 60, no. 2, pp. 681–690, Feb. 2013.
6. Wang F., Li S.,. Mei X, Xie W., Rodriguez J. and Kennel R. M.: "Model-Based Predictive Direct Control Strategies for Electrical Drives: An Experimental Evaluation of PTC and PCC Methods", *IEEE Trans. Ind. Informatics*, vol. 11, no. 3, pp. 671–681, Jun. 2015.

7. Davari S. A., Khaburi D. A. and Kennel R.: "An Improved FCS–MPC Algorithm for an Induction Motor With an Imposed Optimized Weighting Factor", *IEEE Trans. Power Electron.*, vol. 27, no. 3, pp. 1540–1551, Mar. 2012.
8. Villarroel F., Espinoza J. R., Rojas C. A., Rodriguez J., Rivera M. and. Sbarbaro D: "Multiobjective Switching State Selector for Finite-States Model Predictive Control Based on Fuzzy Decision Making in a Matrix Converter", *IEEE Trans. Ind. Electron.*, vol. 60, no. 2, pp. 589–599, Feb. 2013.
9. Falkowski P.: "Predykcyjne algorytmy sterowania przekształtnikiem AC/DC/AC", Bialystok University of Technology, 2013.
10. Mamdouh M., Abido M. A. and Hamouz Z.: "Weighting Factor Selection Techniques for Predictive Torque Control of Induction Motor Drives: A Comparison Study", *Arab. J. Sci. Eng.*, vol. 43, no. 2, pp. 433–445, Feb. 2018.
11. Vazquez S., Rodriguez J., Rivera M., Franquelo L. G., and Norambuena M.: "Model Predictive Control for Power Converters and Drives: Advances and Trends", *IEEE Trans. Ind. Electron.*, vol. 64, no. 2, pp. 935–947, Feb. 2017.
12. Kazmierkowski M. P. and Tunia H.: "Automatic Control of Converter-Fed Drives", *ELSEVIER*, 1994.
13. Stando D., Chudzik P., A. Moradewicz, R. Miśkiewicz: „Sterowanie predykcyjne z modelem silnika indukcyjnego zasilanego z falownika napięcia", *Przegląd Elektrotechniczny*, no. 11, 96-99, 2014. DOI:10.12915/pe.2014.11.27

Accepted for publication 30.10.2018 r.

STEROWANIE PREDYKCYJNE Z OPTYMALNĄ SEKWENCJĄ ŁĄCZEŃ FALOWNIKA TRÓJPOZIOMOWEGO ZASILAJĄCEGO NAPĘD Z SILNIKIEM INDUKCYJNYM KLATKOWYM

Dariusz STANDO, Marian P. KAŹMIERKOWSKI

STRESZCZENIE *W artykule przedstawiono nowatorski system predykcyjnego sterowania z modelem (ang. Model Predictive Control – MPC) bezczujnikowym napędem z silnikiem klatkowym zasilanym z falownika trójpoziomowego pracującego w szerokim zakresie prędkości łącznie z osłabianiem strumienia stojana. Do ważnych zalet opracowanego układu sterowania napędu należą: bardzo wysoka dynamika regulacji momentu i strumienia, stała częstotliwość łączeń falownika i brak konieczności doboru współczynników wag w funkcji kosztów sterowania predykcyjnego. Opisano zasady teoretyczne zastosowanej optymalnej sekwencji łączeń w metodzie sterowania predykcyjnego. Przedstawione wyniki eksperymentalne napędu o mocy 50 kW potwierdzają zalety zaproponowanego systemu sterowania predykcyjnego.*

Słowa kluczowe: *Sterowanie predykcyjne z modelem, Napędy silników indukcyjnych, falowniki trójpoziomowe NPC*